Cis Effects in the Cobalt Corrins. 1. Crystal Structures of 10-Chloroaquacobalamin Perchlorate, 10-Chlorocyanocobalamin, and 10-Chloromethylcobalamin

Kenneth L. Brown,*,† Shifa Cheng,† Xiang Zou,† Jeffrey D. Zubkowski,‡ Edward J. Valente,§ Leanne Knapton,|| and Helder M. Marques*,||

Department of Chemistry, Ohio University, Athens, Ohio 45701, Department of Chemistry, Jackson State University, Jackson, Mississippi 39217, Department of Chemistry, Mississippi College, Clinton, Mississippi 39058, and Centre for Molecular Design, Department of Chemistry, University of the Witwatersrand, PO Wits, 2050 Johannesburg, South Africa

Received December 20, 1996[⊗]

The crystal structures of 10-chloroaquacobalamin perchlorate hydrate (10-Cl-H_2OCbl·ClO_4) (Mo Kα, 0.710 73 Å, monoclinic system, $P2_1$, a = 11.922(4) Å, b = 26.592(10) Å, c = 13.511(5) Å, β = 93.05(3)°, 10 535 independent reflections, R_1 = 0.0426), 10-chlorocyanocobalamin−acetone hydrate (10-Cl-CNCbl) (Mo Kα, 0.710 73 Å, orthorhombic system, $P2_12_12_1$, a = 16.24(3) Å, b = 21.85(5) Å, c = 26.75(8) Å, 7699 independent reflections, R_1 = 0.0698), and 10-chloromethylcobalamin−acetone hydrate (10-Cl-MeCbl) (Mo Kα, 0.71073 Å, orthorhombic system, $P2_12_12_1$, a = 16.041(14) Å, b = 22.13(2) Å, c = 26.75(4) Å, 6792 independent reflections, R_1 = 0.0554), in which the C10 meso H is substituted by Cl, are reported. An unusual feature of the structures is disorder in the C ring, consistent with a two-site occupancy in which the major conformation has the C46 methyl group in the usual position, "upwardly" axial, and the C47 methyl group equatorial, while in the minor conformation both are pseudoequatorial, above and below the corrin ring. ^{13}C NMR chemical shifts of C46, C47, C12, and C13 suggest that the C ring disorder may persist in solution as a ring flip. Since molecular dynamics simulations fail to reveal any population of the minor conformation, the effect is likely to be electronic rather than steric. The axial bond lengths in 10-Cl-MeCbl are very similar to those in MeCbl (d_{Co-C} = 1.979(7) *vs* 1.99(2); to 5,6-dimethylbenzimidazole, d_{Co-NB3} = 2.200(7) *vs* 2.19(2)), but the bonds to the four equatorial N donors, $d_{Co-N(eq)}$, are on average 0.05 Å shorter. In 10-Cl-CNCbl, d_{Co-C} and d_{Co-NB3} are longer (by 0.10(2) and 0.03(1) Å, respectively) than the bond lengths observed in CNCbl itself, while conversely, the C−N bond length is shorter by 0.06(2) Å, but there is little difference in $d_{Co-N(eq)}$. The Co−O bond length to coordinated water in 10-Cl-H_2OCbl$^+$ is very similar to that found in H_2OCbl$^+$ itself, but the d_{Co-NB3} bond is longer (1.967 *vs*1.925-(2) Å), while the average $d_{Co-N(eq)}$ is very similar. The coordinated water molecule in 10-Cl-H_2OCbl$^+$ is hydrogen bonded to the *c* side chain carbonyl oxygen, as in H_2OCbl$^+$. NMR observations indicate that the H bond between coordinated H_2O and the *c* side chain amide persists in solution. The equilibrium constant, K_{Co}, for coordination of bzm to Co(III) is smaller in 10-Cl-MeCbl and 10-Cl-CNCbl than in their C10-unsubstituted analogs (181 *vs* 452; 4.57 × 10^3 *vs* 3.35 × 10^5), but could not be determined for 10-Cl-H_2OCbl because hydrolysis of the phosphodiester is competitive with the establishment of the base-off equilibrium. Substitution of H by Cl at C10 causes the bands in the electronic spectrum of 10-Cl-XCbl complexes to move to lower energy, which is consistent with an increase in electron density in the corrin π-conjugated system. This increased electron density is not due to greater electron donation from the axial ligand as bonds between these and the metal are either longer (not shorter) or unchanged, and it most probably arises from π-donation to the corrin by Cl at C10. As the donor power of X increases (H_2O < CN^- < Me), the corrin ring becomes more flexible to deformation, and the number of bond lengths and bond angles that are significantly different in XCbl and 10-Cl-XCbl increases; importantly, the C10−Cl bond length, d_{C10-Cl}, increases as well. Thus, despite the fact that chlorine is an inductively electron withdrawing substituent, its resonance electron donation is the more important effect on electron distribution in the corrin ring. Mulliken charges obtained from semiempirical RHF-SCF MO calculations using the ZINDO/1 model on XCbl and their 10-Cl analogs at the crystal structure geometry are shown to correlate reasonably well with ^{13}C NMR shifts and may be used to determine the pattern of electron distribution in these complexes. Substitution by Cl at C10 causes an increase in charge density at Co when X = H_2O and CN^-, while the charge density on the four equatorial N donors remains virtually unchanged, but a decrease when X = Me, while the charge density on the equatorial N donors also decreases. In response, d_{Co-NB3} increases in the first two complexes but the equatorial bond lengths remain virtually unchanged, while d_{Co-NB3} remains unchanged and the average $d_{Co-N(eq)}$ decreases in 10-Cl-MeCbl. Furthermore, the partial charge on chlorine increases as the donor power of X increases. The small decrease in the pK_a of coordinated H_2O in 10-Cl-H_2OCbl$^+$ compared to H_2OCbl$^+$ itself (7.65 *vs* 8.09) is due to a decreased charge density on oxygen in 10-Cl-OHCbl compared to OHCbl. The picture that emerges, therefore, is of competitive electron donation by X and Cl toward the corrin system. In 10-Cl-CNCbl, the decrease in the C≡N bond length as Co−C increases compared to CNCbl suggests that dπ−pπ bonding between cobalt and cyanide is important. ^{13}C and ^{15}N NMR observations on 10-Cl-^{13}C^{15}NCbl are consistent with these effects.

Introduction

While Co(III) is a classical example of an inert transition metal ion, the Co(III) center of the cobalt corrins is remarkably labile toward axial ligand substitution. A comparison of representative second-order rate constants for substitution by an incoming ligand, L, of H_2O in Co(III) complexes with four N-donor equatorial ligands (N_4) (eq 1) shows that the ap-

$$X-Co^{III}(N_4)-OH_2 + L \xrightarrow{k_2} X-Co^{III}(N_4)-L + H_2O \quad (1)$$

proximate lability ratio of the metal ion toward substitution in

† Ohio University.
‡ Jackson State University.
§ Mississippi College.
|| University of the Witwatersrand.
⊗ Abstract published in *Advance ACS Abstracts,* August 1, 1997.

S0020-1669(96)01507-8 CCC: $14.00

Table 1. Rate Constants for Some Ligand Substitution Reactions in $Co^{III}(N_4)$ Complexes[a]

$$X-Co^{III}(N_4)-OH_2 + L \rightarrow X-Co^{III}(N_4)-L + H_2O$$

X	N_4	L	$k_2/M^{-1}\,s^{-1}$	ref
OH^-	corrin	N_3^-	1.6×10^5	1
OH^-	porphyrin[b]	N_3^-	7.2×10^2	2
H_2O	corrin	I^-	2.2×10^3	3
H_2O	porphyrin[b]	I^-	1.62	4
I^-	corrin	SCN^-	1.5×10^2	3
I^-	cobaloxime[c]	SCN^-	1.2×10^{-3}	5
H_2O	corrin	SCN^-	8.2×10^2	3
H_2O	$(NH_3)_4$	SCN^-	8.6×10^{-7}	6

[a] Substitution of coordinated H_2O (eq 1). [b] Tetrakis(4-*N*-methylpyridyl)porphinato. [c] Bis(dimethylglyoximato).

corrin, porphyrin, cobaloxime, and ammine systems is 10^9:10^6:10^4:1 (Table 1). By factoring out steric effects, Poon[7] has demonstrated that rate constants for the hydrolysis of $Co^{III}(N_4)$ complexes (eq 2) increase with the extent of unsaturation of the equatorial ligand, varying in the ratio 1:36:270 as N_4 is changed from cyclam, to *trans*[14]diene, to cobaloxime.[8] These

$$Cl-Co^{III}(N_4)\text{-}Cl + H_2O \xrightarrow{k_1} Cl-Co^{III}(N_4)-OH_2 + Cl- \quad (2)$$

labilization effects suggest a substantial kinetic *cis* effect by the equatorial ligands through to the axial coordination site. There also appears to be a significant ground state structural *cis* effect. In diaqua complexes (H_2O *trans* to H_2O) of cobalt(III)(tetraphenylporphine), the Co−O bond lengths are 1.932 and 1.939 Å,[9] but only 1.913 Å in the macrocycle Me_4[14]tetraene;[10] the Co−O bond length in cobyric acid[11] (H_2O trans to CN^-) is 2.065 Å, but in aqua(cyano)cobaloxime it is significantly shorter (1.992 Å);[12] and in aquacobalamin (H_2O *trans* to bzm) the Co−O bond length is 1.952[13] or 1.961,[14] but in aqua(pyridine)cobaloxime it is 1.916 Å.[15]

These kinetic and the structural *cis* effects could be a consequence of the delocalization of electron density from the equatorial ligands onto the metal ion. This would impart some Co(II)-like character to Co(III) and so explain the kinetic lability of, and the longer axial bond lengths to, the "Co(III)" center in systems with unsaturated equatorial ligands. It should be noted, however, that these effects are modest when compared to a full one-electron reduction of the metal ion. Thus, the rate constant for exchange of H_2O, k_{ex}, in $[Co^{III}(NH_3)_5(OH_2)]^{3+}$ at 25 °C is $5.9 \times 10^{-6}\ s^{-1}$,[16] but in $[Co^{II}(NH_3)_2(OH_2)_4]^{2+}$ it is 13 orders of magnitude larger, $6.5 \times 10^7\ s^{-1}$,[17] and even in an associative reaction on the sterically-crowded tetramethylcyclam, $[Co^{II}(tmc)(OH_2)]^{2+}$, $k_{ex} = 4.2 \times 10^4\ s^{-1}$.[18] The second-order rate constants for anation of $[Co^{III}(NH_3)_5(OH_2)]^{3+}$ at 25 °C by SCN^- and Cl^- are 6.9×10^{-6} and $6.5 \times 10^{-5}\ M^{-1}\ s^{-1}$, respectively,[19] but the second-order rate constants are 2.3×10^3, 4.9×10^3, and $1.6 \times 10^4\ M^{-1}\ s^{-1}$ for anation of $[Co^{II}(tmc)(OH_2]^{2+}$ by OCN^-, SCN^-, and N_3^-, respectively.[20] Reduction of methylcobalamin results in a $>10^{15}$ rate enhancement of thermal homolysis of the Co−C bond,[21] while Co(II) corrins such as cobalt(II) cobyrinate[22] and cob(II)alamin[23] are five-coordinate: one of the axial ligands is entirely absent or, at most,[23] interacts very weakly with the metal center. Consequently, the conferring of even relatively slight Co(II) character by the equatorial ligand in a $Co^{III}(N_4)$ complex could have a very substantial kinetic labilizing effect.

The dissociation of the Co−C bond is now widely recognized to be the primary event in the adenosylcobalamin-dependent enzyme catalytic cycle. It has been suggested[24] that the homolysis may be triggered by a conformationally-induced distortion of the corrin ring toward the 5′-deoxyadenosyl ligand, and that one reason Nature employs the corrin macrocycle is the insufficient flexibility of other possible macrocycles, such as a porphyrin, for this purpose.[25] However, there is now quite extensive evidence of the extraordinary flexibility of the porphyrin ring.[26] It is tempting to speculate that one of the functions of the corrin in the cobalt corrins is to impart lability on the Co(III) center, for which the corrin appears more suited than the porphyrin (Table 1). Questions such as this have prompted us to begin a study of *cis* effects in cobalt corrins, on both the structural and kinetic levels. In the present paper, we report on the molecular structures of 10-chloromethylcobalamin

(1) Marques, H. M.; Bradley, J. C.; Brown, K. L.; Brooks, H. *J. Chem. Soc., Dalton Trans.* **1993**, 3475.
(2) Pasternack, R. F.; Gillies, B. S.; Stromsted, J. P. *Bioinorg. Chem.* **1978**, *8*, 33.
(3) Betterton, E. A. Ph.D. Thesis, University of the Witwatersrand, Johannesburg, South Africa, 1982.
(4) Ashley, K. R.; Berggren M.; Cheng, M. *J. Am. Chem. Soc.* **1975**, *97*, 1422.
(5) Hague D. N.; Halpern, J. *Inorg. Chem.* **1967**, *6*, 2059.
(6) Jackson, W. G.; Jurisson, S. S.; McGregor, B. C. *Inorg. Chem.* **1985**, *24*, 1788.
(7) Poon, C. K. *Coord. Chem. Rev.* **1973**, *10*, 1.
(8) (a) Abbreviations used: AdePrCbl, adenylpropylcobalamin; AdoCbl, 5′-deoxyadenosylcobalamin; MeCbl, methylcobalamin; CNCbl, cyanocobalamin; CN-13-*epi*-Cbl, cyano-13-*epi*-cobalamin; CN-8-*epi*-Cbl, cyano-8−*epi*-cobalamin; H_2OCbl^+, aquacobalamin; 10-Cl-CNCbl, 10-chlorocyanocobalamin; 10-Cl-H_2OCbl^+, 10-chloroaquacobalamin; bzm, 5,6-dimethylbenzimidazole; cobaloxime, bis(dimethylglyoximato); *trans*[14]diene, 1,4,8,11-tetraazacyclotetradeca-1,7-diene; cyclam, 1,4,8,-11-tetraaza-*cyclo*-tetradecane; tmc, 1,4,8,11-tetramethylcyclam; MPA, Mulliken population analysis; MD, molecular dynamics; MM, molecular mechanics; *H* is the generalized acidity function.[8b] (b) Cox, R. P.; Yates, K. *J. Am. Chem. Soc.* **1978**, *100*, 3861.
(9) Masuda, H.; Taya, T.; Osaki, K.; Sugimoto, H.; Mori, M. *Bull. Chem. Soc. Jpn.* **1982**, *55*, 4.
(10) Endicott, J. F.; Durham, D.; Glick, M. D.; Anderson, T. J.; Kuszaj, J. M.; Schmonsees, W. G.; Balakrishnan, K. P. *J. Am. Chem. Soc.* **1981**, *103*, 1431.
(11) Venkatesan, K.; Dale, D.; Hodgkin, D. C.; Nockolds, C. E.; Moore F. H.; O'Connor, B. H. *Proc. R. Soc. London, Ser. A* **1971**, *A323*, 455.
(12) Alvarez S.; Lopez, C. *Inorg. Chim. Acta* **1982**, *64*, L99.
(13) Kratky, C.; Färber, G.; Gruber, K.; Wilson, K.; Dauter, Z.; Nolting, H.-F.; Konrat, R.; Kräutler, B. *J. Am. Chem. Soc.* **1995**, *117*, 4654.
(14) Brown, K. L.; Evans, D. R.; Zubkowski, J. D.; Valente, E. J. Unpublished.
(15) Attia, M. W.; Zangrando, E.; Randaccio, L.; Lopez, C. *Acta Crystallogr., Sect. C* **1987**, *C43*, 1521.
(16) Hunt, H. R.; Taube, H. *J. Am. Chem. Soc.* **1958**, *80*, 2642.
(17) West, R. J.; Lincoln, S. F. *Inorg. Chem.* **1973**, *12*, 494.
(18) Meier, P.; Merbach, A.; Bürki, S.; Kaden, T. A. *J. Chem. Soc., Chem. Commun.* **1976**, 36.
(19) Langford, C. H.; Muir, W. R. *J. Am. Chem. Soc.* **1967**, *89*, 3141.
(20) Bürki, S.; Kaden, T. A. *J. Chem. Soc., Dalton Trans.* **1991**, 805.
(21) Martin, B. D.; Finke, R. G. *J. Am. Chem. Soc.* **1992**, *114*, 585.
(22) Kräutler, B; Keller, W.; Hughes, M.; Caderas, C.; Kratky, C. *J. Chem. Soc., Chem. Commun.* **1987**, 1678.
(23) Kräutler, B; Keller, W.; Kratky, C. *J. Am. Chem. Soc.* **1989**, *111*, 8936.
(24) (a) Toraya, T.; Ishida, A. *Biochemistry* **1988**, *27*, 7677. (b) Halpern, *J. Bull. Soc. Chim. Fr.* **1988**, 187. (c) Pett, V. B.; Liebman, M. N.; Murray-Rust, P.; Prasad, K.; Glusker, J. P. *J. Am. Chem. Soc.* **1987**, *109*, 3207. (d) Pratt, J. M. *Pure Appl. Chem.* **1993**, *65*, 1513. (e) Waddington, M. D.; Finke, R. G. *J. Am. Chem. Soc.* **1993**, *115*, 4629.
(25) Geno, M. K.; Halpern, J. *J. Am. Chem. Soc.* **1987**, *109*, 1238.
(26) (a) Senge, M. O. *J. Photochem. Photobiol.* **1992**, *B16*, 3. (b) Munro, O. Q.; Bradley, J. C.; Hancock, R. D.; Marques, H. M.; Marsicano, F.; Wade, P. W. *J. Am. Chem. Soc.* **1992**, *114*, 7218. (c) Melamed, D.; Spiro, T. G. *J. Phys. Chem.* **1993**, *97*, 7441. (d) Sparks, L. D.; Anderson, K. K.; Medforth, C. J.; Smith, K. M.; Shelnutt, J. A. *Inorg. Chem.* **1994**, *33*, 2297. (e) Medforth, C. J.; Muzzi, C. M.; Smith, K. M.; Abraham, R. J.; Hobbs, J. D.; Shelnutt, J. A. *J. Chem. Soc., Chem. Commun.* **1994**, 1843. (f) Nakamura, M. *Bull. Chem. Soc. Jpn.* **1995**, *68*, 197. (g) Senge, M. O.; Ema T.; Smith, K. M. *J. Chem. Soc., Chem. Commun.* **1995**, 733. (h) Ravikanth M.; Chandrashekar, T. K. *Struct. Bonding (Berlin)* **1995**, *82*, 105. (i) Munro, O. Q.; Marques, H. M.; Debrunner, P. G.; Mohanrao K.; Scheidt, W. R. *J. Am. Chem. Soc.* **1995**, *117*, 935.

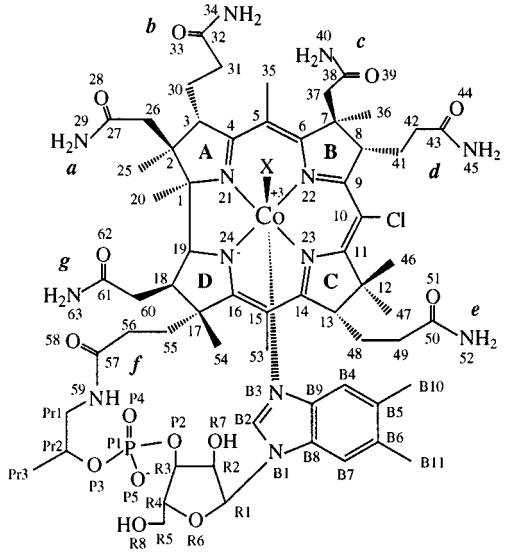

Figure 1. Numbering scheme for 10-chlorocobalamins. For 10-Cl-MeCbl, 10-Cl-CNCbl, and 10-Cl-H_2OCbl$^+$, X = Me, CN^-, and H_2O, respectively. MeCbl, CNCbl, and H_2OCbl$^+$ have H at C10.

(10-Cl-MeCbl), 10-chlorocyanocobalamin (10-Cl-CNCbl), and 10-chloroaquacobalamin (10-Cl-H_2OCbl$^+$) determined by X-ray diffraction methods (Figure 1).

Experimental Section

Synthesis of 10-Cl-MeCbl from MeCbl. MeCbl (*vide infra*, 100 mg, 74 μmol) was dissolved in 10 mL of water; 100 μL of glacial acetic acid was added, followed by a slow addition of 1.2 equiv of chloramine-T hydrate (Sigma, 97%) in 20 mL of water. After 60 min, the solution was concentrated to a small volume and the product was separated by semipreparative HPLC (82 mg, 80% yield). The ^{13}C NMR spectrum was tentatively assigned (Table S1 of the Supporting Information) by analogy with the assignments of MeCbl.[27] An overlay of the electronic spectra of 10-Cl-MeCbl and MeCbl is shown in Figure 2A. λ/nm (log ϵ): 285 (4.28), 291 (4.28), 347 (4.20), 374 (4.11), 500 (sh), 543 (3.91).

Synthesis of 10-Cl-CNCbl from CNCbl. (a) 10-Cl-CNCbl-*c*-lactone.[28] To CNCbl (100 mg, 74 μmol, Roussel) dissolved in 100 mL of water and 10 mL of 1.0 M HCl was slowly added about 2.5 equiv of chloramine-T hydrate in 50 mL of water. The reaction mixture was desalted on an Amberlite XAD-2 column, and the product was eluted with 10% (v/v) MeCN/H_2O (90% yield). The ^{13}C NMR spectrum was tentatively assigned (Table S2 of the Supporting Information) by analogy with the assignments of 10-Cl-CNCbl (*vide infra*) and CNCbl-*c*-lactone.[29]

(b) 10-Cl-CNCbl-*c*-COO$^-$.[29] 10-Cl-CNCbl-*c*-lactone (100 mg, 72 μmol) was dissolved in 30 mL of 10% (w/w) NH_4Cl solution. The solution was deoxygenated for 60 min (Ar), anaerobically transferred into a deoxygenated flask containing freshened Zn wool, and reduced overnight. The solution was transferred into 50 mL of 0.1 M HCl solution, exposed to air for several hours, and then desalted on an Amberlite XAD-2 column, and the product was eluted with 10% (v/v) MeCN/H_2O (85% yield). The ^{13}C NMR spectrum (Table S2 of the Supporting Information) was tentatively assigned by analogy to that of 10-Cl-CNCbl (*vide infra*) and CNCbl-*c*-COO$^-$.[29] The absence of the *c* side chain amide was confirmed in the ^{15}N NMR spectrum obtained by ^{1}H−^{15}N HMQC spectroscopy (Table S3 of the Supporting Information).

(c) 10-Cl-CNCbl, Method 1.[29] 10-Cl-CNCbl-*c*-COO$^-$ (240 mg, 170 μmol) was dissolved in 80 mL of water; 17.2 g (2000 equiv) of NH_4Cl was added, and the pH was adjusted to 5.9. To this was added 3.5 g (>1000 equiv) of 1-ethyl-3-(3-(dimethylamino)propyl)carbodiimide hydrochloride (EDAC, Sigma), and the reaction was allowed to proceed overnight. HPLC analysis showed 65% conversion to 10-Cl-CNCbl and 35% to the acylurea intermediate, which can be converted back to 10-Cl-CNCbl-*c*-COO$^-$ by treatment with base. UV−vis molar absorptivities were determined by drying crystals from the same crop as used for the X-ray diffraction study at 80 °C over P_2O_5 to constant weight, and preparing weight−volume solutions in deioinized water. The molar absorptivities were determined from a slope of a Beer's law plot. λ/nm (log ϵ): 282 (4.12), 289 (4.14), 364 (4.48), 546 (3.89), 576 (3.93); for 10-Cl-$(CN)_2$Cbl, $\epsilon_{370} = (3.41 \pm 0.02) \times 10^4$ M^{-1} cm^{-1}. An overlay of the electronic spectra of 10-Cl-CNCbl and CNCbl is shown in Figure 2B. FAB MS: Calcd for M$^+$ for 10-Cl-CNCbl 1389.5, found 1389.7. The ^{1}H and ^{13}C NMR spectra were unambiguously assigned using homonuclear and heteronuclear 2D NMR methods.[30] The complete NMR correlations are given in Table S4 of the Supporting Information, and the ^{1}H and ^{13}C NMR assignments are given in Table S5. The ^{1}H−^{15}N spectrum was readily assignable by analogy to that of CNCbl,[25] and the amide ^{1}H and ^{15}N chemical shifts are given in Table 2.

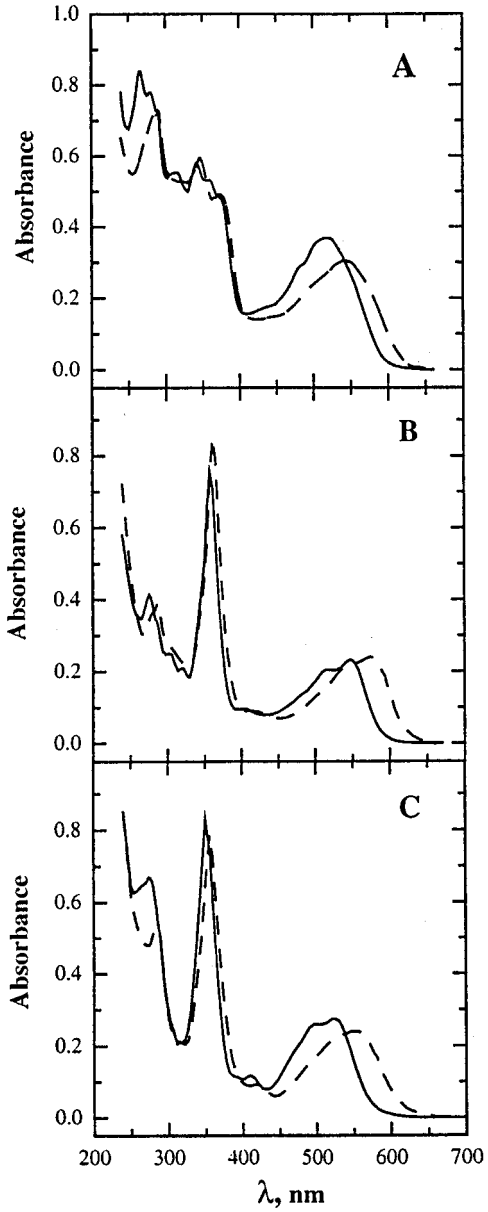

Figure 2. UV−visible spectra of (A) 2.0 × 10^{-5} M (—) MeCbl and (- - -) 10-Cl-MeCbl, (B) 2.78 × 10^{-5} M CNCbl (—) and 10-Cl-CNCbl (- - -), and (C) 3.20 × 10^{-5} H_2OCbl$^+$ (—) and 10-Cl-H_2OCbl$^+$ (- - -).

(27) Brown, K. L.; Evans, D. R.; Zubkowski, J. D.; Valente, E. J. *Inorg. Chem.* **1996**, *35*, 415.
(28) Bonnett, R.; Cannon, J. R.; Clark, V. M.; Johnson, A. W.; Parker, L. F. J.; Lester-Smith, E.; Todd, A. *J. Chem. Soc.* **1957**, 1158.
(29) Brown, K. L.; Cheng, S.; Marques, H. M. *Inorg. Chem.* **1995**, *34*, 3038.
(30) Brown, K. L.; Zou, X.; Wu, G.-Z.; Zubkowski, J. D.; Valente, E. J. *Polyhedron* **1995**, *14*, 1621.

Table 2. Amide ^{15}N and ^{1}H Chemical Shifts for 10-Cl-XCbl (X = CN^-, H_2O)[a]

	10-Cl-CNCbl		10-Cl-H_2OCbl$^+$			
amide	$\delta_{^{15}N}$/ppm[b]	$\delta_{^{1}H}$/ppm[c]	$\delta_{^{15}N}$/ppm[b]	$\delta_{^{1}H}$/ppm[c]	$\Delta\delta_{^{15}N}$/ppm[d]	$\Delta\delta_{^{1}H}$/ppm[d]
a	115.9	7.14, 7.86	116.4	7.14, 7.86	0.5	0.00, 0.00
b	109.5	6.92, 7.64	109.7	6.93, 7.65	0.2	0.01, 0.01
c	114.8	7.03, 7.54	118.4	7.11, 8.08	3.6	0.08, 0.54
d	106.7	6.35, 6.56	107.0	6.38, 6.56	0.3	0.03, 0.00
e	110.0	7.03, 7.75	110.3	7.04, 7.77	0.3	0.01, 0.02
f	118.0	8.20	118.6	8.21	0.6	0.01
g	111.4	7.10, 7.96	111.5	7.11, 7.94	0.1	0.01, −0.02

[a] In 10% D_2O/90% H_2O at 300 K. [b] Chemical shifts referenced to external CH_3NO_2 but reported relative to NH_3(l) ($\delta_{CH_3NO_2}$ = 380.23 ppm). [c] Chemical shifts relative to external TSP. [d] $\Delta\delta = \delta_{10-Cl-H_2O} - \delta_{10-Cl-CNCbl}$.

Synthesis of 10-Cl-H_2OCbl·ClO_4 from CNCbl. (a) MeCbl. CNCbl (200 mg, 148 μmol) was dissolved in 35 mL of 10% (w/w) aqueous NH_4Cl solution. After deaeration (Ar) in the dark for 40 min, freshened Zn wool was added in excess. The reduction was monitored by HPLC, and on completion, 200 μL of MeI (Aldrich) was injected. After 30 min, the solution was transferred into 30 mL of 1 mM HCl, exposed to air, and desalted on an Amberlite XAD-2 column (quantitative yield).

(b) 10-Cl-CNCbl, Method 2. 10-Cl-MeCbl in acidic solution was exposed to light for several hours. The solution was neutralized, and an excess of KCN was added to convert all corrins to their dicyano complexes. The mixture was loaded onto an Amberlite XAD-2 column and washed with 10 column volumes of 1 mM HCl to convert 10-Cl-$(CN)_2$Cbl to 10-Cl-CNCbl. Elution and then purification by HPLC yielded 10-Cl-CNCbl in *ca.* 90% yield.

(c) 10-Cl-H_2OCbl·ClO_4. 10-Cl-CNCbl (50 mg, 36 μmol) was dissolved in 30 mL of 10% (w/w) aqueous NH_4Cl solution and deaerated (Ar) for 2 h. This was anaerobically transferred to an Ar-purged flask and contacted with freshened Zn wool. Ar was bubbled vigorously through the solution for 5 h to remove HCN. The reaction was monitored at regular intervals by HPLC until complete conversion had occurred. The solution was then transferred into 50 mL of 0.1 M HCl, contacted with air for several hours, and desalted on an Amberlite XAD-2 column. No further purification was required after elution with 50% (v/v) MeCN/H_2O. The chloride salt of 10-Cl-H_2OCbl$^+$ could also be quantitatively prepared by photolyzing 10-Cl-MeCbl in acidic solution followed by the usual workup procedures. The ^{13}C NMR spectrum was tentatively assigned (Table S2 of the Supporting Information) by analogy with the assignments of 10-Cl-CNCbl and H_2-OCbl$^+$. A solution of the chloride salt of 10-Cl-H_2OCbl$^+$ was loaded onto a column packed with Sephadex CM cation exchange resin which had been previously washed with copious quantities of deioinized water. After washing with water, the colored band was eluted from the column with 1.0 M $KClO_4$. The eluent was desalted on an Amberlite XAD-2 column and eluted with 50% (v/v) MeCN/H_2O. UV−vis molar absorptivities were determined by dissolution of crystals from the same crop as used for the X-ray diffraction study. λ/nm (log ϵ): 280 (4.20), 357 (4.40), 527 (3.83), 554 (3.87). An overlay of the electronic spectra of 10-Cl-CNCbl and CNCbl is shown in Figure 2C.

NMR Spectroscopy. One-dimensional ^1H and ^{13}C NMR spectra were obtained on a GE QE 300 NMR spectrometer. Two-dimensional homonuclear (COSY, TOCSY, and ROESY) and $^1H-^{13}C$ heteronuclear (HMQC and HMBC) spectra were obtained on a Bruker AMX 600 NMR spectrometer and interpreted as described previously.[30] Inverse-detected $^1H-^{15}N$ HMQC spectra were obtained on a Bruker AMX 300 NMR spectrometer as described previously.[31,32] For detection of the amide nitrogen resonances, the coupling delay was set to 5.6 ms ($^1J_{NH}$ = 90 Hz), while the B1 and B3 nitrogens of the axial nucleotide were detected at the B2 hydrogen using a coupling delay of 68 ms ($^2J_{NH}$ = 7.4 Hz).[32b]

X-ray Crystallography. Crystals of 10-Cl-MeCbl, 10-Cl-CNCbl, and 10-Cl-H_2OCbl·ClO_4 were obtained by vapor diffusion of acetone into aqueous solutions of the compound. X-ray diffraction measurements were carried out on a Siemens R3m/V diffractometer using graphite-monochromated Mo Kα radiation (λ = 0.710 3 Å) at T = 295(2) K.

10-Cl-MeCbl. A thin prismatic rod-like crystal of dimensions 0.5 × 0.2 × 0.8 mm was mounted in contact with acetone in a 0.5 mm glass capillary and sealed with wax. A preliminary examination with Mo Kα radiation showed the crystals to belong to the orthorhombic system, space group $P2_12_12_1$. Cell constants and information on the data collection and refinement are given in Table S6 of the Supporting Information. Data were collected by ω scans of 2.0° width with three standard reflections monitored after every 97 reflections. No deterioration was found over the course of the 100 h data collection period. A total of 6792 unique data were collected comprising a complete octant to 2θ = 45.0°. The solution of the structure proceeded from the atom positions of 10-Cl-CNCbl (*vide infra*). Positions and anisotropic vibrational terms for non-H atoms of the cobalamin (except for disordered atoms, see Supporting Information) were refined by damped full-matrix least squares computations.[33] H atoms (with isotropic vibrational factors set to 120% of the equivalent isotropic vibrational factor for the attached non-H atom) were placed in calculated positions and allowed to ride on their attached non-H atoms, but H atoms of the ribose hydroxyl groups were located and refined (although with fixed isotropic vibrational factors). Details for ordered and partially-ordered water molecules are given in the Supporting Information.

The positions of the C ring carbon atoms C12, C46, and C47 were found disordered over two alternate orientations (refined occupancy value of the major component was 0.737(8)), corresponding to alternate envelope flap orientations of the C ring. The positions of the geminal methyl carbon atoms and the flap carbon C12 were refined with isotropic vibrational factors, and the H atom at C13 was modeled in each likely conformational location. The *c* side chain (C41, C42, C43, O44, and N45) was found in two orientations (occupancy of the major conformer 0.707(6)), both of which were modeled with isotropic non-H atoms. The elongated vibrational ellipsoids of C7, C8, and C9 suggest additional disorder in this region, but this could not be resolved. Methyl H atoms on C35, C53, and C10B were disordered over equivalent trigonal positions. The likely H-bond contacts between cobalamin donor and acceptor atoms are given in the Supporting Information.

10-Cl-CNCbl. A thin rod-like crystal, 1.0 × 0.23 × 0.08 mm, was wedged into a 0.2 mm glass capillary containing a column of acetone and sealed with silicone grease. Centering of 27 reflections for which $2\theta > 25°$ gave the orthorhombic space group $P2_12_12_1$ (Table S6). A total of 9978 reflections were observed; three standard reflections (0,2,−5; 3,2,0; 0,−4,0) were observed every 97 reflections, and their mean intensity over the course of the data collection was 0.997 of the first intensities. Corrections were applied for coincidence, Lorentz, and polarization effects, but not for deterioration or decomposition. No absorption correction was required. Data were collected to θ = 21.5°. Equivalent data were merged, R_{int} = 0.0418. The structure was discovered by computing the Patterson function. A peak at 0.237, 0.596, 0.744 was assigned to cobalt, and the remainder of the cobalamin was assembled in stages by computing difference Fourier maps. On location of the non-H atoms of the cobalamin, water oxygen locations were found by accepting difference map peaks in likely H-bonding positions from donor or acceptor atoms and other water molecules.

(31) Brown, K. L.; Evans, D. R. *Inorg. Chem.* **1993**, *32*, 2544.
(32) (a) Brown, K. L.; Zou, X. *J. Am. Chem. Soc.* **1993**, *115*, 1478. (b) Brown, K. L.; Evans, D. R.; Zou, X.; Wu, G.-Z. *Inorg. Chem.* **1993**, *32*, 4487. (c) Brown, K. L.; Evans, D. R. *Inorg. Chem.* **1994**, *33*, 525.
(33) Sheldrick, G. M. *SHELXL-93, Program for Crystal Structure Determination*; University of Göttingen, 1993.

Full-matrix least squares refinement on F^2 was carried out using SHELXL-93.[33] Non-H atoms were allowed to refine with their anisotropic vibrational factors; H atoms were placed, allowed to contribute but not refined.

As was the case for 10-Cl-MeCbl, elongated vibrational ellipsoids were noticed for C12, C46, and C47, consistent with disorder in the C ring between two conformations. The atoms of the major and minor conformations were refined with anisotropic and isotropic vibrational factors, respectively. H atoms with appropriate site occupancies were placed at calculated positions and assigned isotropic factors. The major conformation refined to a site occupancy of 0.78(2). Isotropic and equivalent isotropic vibrational factors for corresponding atoms agree. Details of ordered and disordered water molecules are given in the Supporting Information.

10-Cl-H_2OCbl·ClO_4. A thin block crystal, 0.4 × 0.4 × 0.08 mm, was mounted in a 0.4 mm glass capillary containing a column of acetone and sealed with silicone grease. Centering of 30 reflections, 12.5° < θ < 23.5°, gave the monoclinic space group $P2_1$ (Table S6). A total of 11 685 reflections, including standard monitors, were observed, from which 10 534 unique data were obtained. An empirical absorption correction was calculated and applied.[34] The structure was discovered by applying the Patterson function, from which preliminary locations of Co, P, and two Cl atoms could be discerned. The rest of the model was built by successive cycles of Fourier and least squares calculations using SHELXL-93.[33]

A disorder in the positions of C12, C46, and C47 was found. As for 10-Cl-MeCbl and 10-Cl-CNCbl, this could be modeled as an equilibrium between two conformations of the C ring with C46 axial and C47 equatorial in the major conformation (0.75(1)). H atom positions were calculated (except for H's on O7R, O8R, and one water molecule which were fitted to likely H-bonded locations). H atoms at C10, C11, C35, C36, and C53 were found trigonally disordered, and the alternative positions were included in the model.

Complete details are given in the Supporting Information, as are atomic coordinates of 10-MeCbl, 10-Cl-CNCbl, and 10-Cl-H_2OCbl·ClO_4, anisotropic temperature factors, bond angles and bond distances between adjacent non-hydrogen atoms, and calculated hydrogen atom coordinates.

The pK_as of 10-Cl-MeCbl, 10-Cl-CNCbl, and 10-Cl-H_2OCbl$^+$. The pK_a of coordinated water in H_2OCbl$^+$ and in 10-Cl-H_2OCbl$^+$ was determined by spectrophotometric titration in 1 cm path length cells in the thermostated cell holder of a Cary 3E spectrometer at 355 and 565 nm using 20−25 μM solutions with I = 0.5 M ($NaNO_3$), 0.01 M Tris/HNO_3 buffer, between 5.0 and 35 °C. The pH of the solutions was measured using a Metrohm 6.0210.000 glass electrode calibrated against standard buffers. The data were fitted using standard nonlinear least squares procedures, and ΔH and ΔS were determined from plots of ln K_a against 1/T by linear least squares.

The p$K_{base-off}$ for the base-off ⇌ base-on equilibrium of 10-Cl-MeCbl (eq 3) was determined spectrophotometrically at 560 nm using a 1.5 × 10^{-4} M solution at 25.0 °C as described previously.[35] Plots of absorbance against pH were fitted by nonlinear least squares methods to yield p$K_{base-off}$ = 3.30 ± 0.01. A similar titration for 10-Cl-CNCbl (1.5 × 10^{-4} M, 592 nm, 25.0 °C) gave p$K_{base-off}$ = 1.87 ± 0.03. Plotting the data as a Henderson−Hasselbalch plot of log(α/(1−α)), where α is the fraction of base-on species, against pH gave p$K_{base-off}$ = 1.93 ± 0.02, i.e., p$K_{base-off}$ = 1.90 ± 0.04.

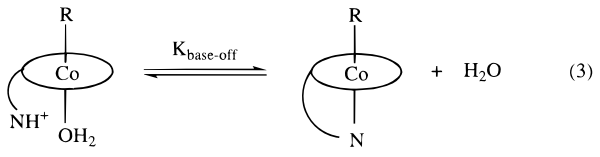

(3)

The p$K_{base-off}$ for 10-Cl-H_2OCbl$^+$ could not be determined. The rate for release of bzm from H_2OCbl$^+$ is slow.[36] In a high acidity solution (H = −3), spectral equilibration of a solution of 10-Cl-H_2OCbl$^+$ took 15 h, which implies that the equilibrium is achieved even more slowly than with H_2OCbl$^+$. At H = −6, equilibration occurred much faster. Since the approach to the off/on equilibrium should become slower with increasing acidity, limiting the off rate at k_{off} of bzm, and since the phosphodiester linkage is hydrolyzed slowly in acid,[37] this suggests that phosphodiester hydrolysis competes with the off/on equilibrium.

Molecular Modeling. Molecular dynamics (MD) simulations of CNCbl were performed using the potential functions of the molecular mechanics (MM) program MM2[38] and the force field developed for the cobalt corrins[39] with HYPERCHEM version 4.5.[40] Simulations were performed at 300 K for 100 ps with data sampling every 1 fs. RHF-SCF MO calculations were performed using the ZINDO/1 model[41] with HYPERCHEM version 4.5 as single-point calculations at the crystal structure geometry of XCbl and 10-Cl-XCbl (X = Me, CN^-, H_2O) with H atoms placed in standard positions. The structures of OHCbl and 10-Cl-OHCbl were obtained by removing the non-hydrogen-bonded proton from coordinated H_2O in H_2OCbl$^+$ and 10-Cl-H_2OCbl$^+$.

Results

Crystal Structure of 10-Cl-MeCbl. 10-Cl-MeCbl, like its C10-unsubstituted analog, MeCbl,[42] crystallizes in the orthorhombic space group $P2_12_12_1$ (R_1 = 5.54%, Figure 3A). Figure 4A shows an overlay of MeCbl and 10-Cl-MeCbl. Even though the available structure of MeCbl is not very precise (R_1 = 14.6%), many significant differences in bond lengths and bond angles between the two structures are apparent. These are summarized in Table S7 of the Supporting Information, and a full comparison is given in Tables S8 and S9 of the Supporting Information. The axial bond lengths to methyl and bzm are identical, within experimental error, but the bonds between cobalt and N21, N22, and N23 are all substantially shorter (Table 3). The corrin fold angle and the base tilt angle are given in Table 4. The corrin is somewhat less folded, and the base less tilted, in 10-Cl-MeCbl than in MeCbl, although the differences are small.

The disorder in the *d* side chain is not surprising, as we have previously shown,[39] using MM calculations, that a number of conformations are available to the side chains of the corrins. More unexpected is the disorder in the C ring, with the ring in two alternative envelope conformations. The major conformation has C46 and C47 in the usual axial and equatorial orientations, respectively, while in the minor conformation C46 and C47 are both in pseudoequatorial positions, above and below the plane of the C ring, respectively (Figure 4).

Crystal Structure of 10-Cl-CNCbl. 10-Cl-CNCbl crystallizes in the orthorhombic space group $P2_12_12_1$ (R_1 = 6.98%, Figure 3B). Although the structures of CNCbl and 10-Cl-CNCbl are similar (Figure 4B), a number of bond lengths and bond angles differ (Tables S7, S10, and S11); there are significantly fewer differences between CNCbl and 10-Cl-CNCbl than between MeCbl and 10-Cl-MeCbl, however. The Co−C bond length of coordinated cyanide is 1.96(2) Å, significantly longer than the 1.86(1) Å observed in CNCbl;[43]

(34) *SHELEXA-90*, version 1; Siemens Analytical X-ray Instruments, Inc.: Madison, WI.
(35) Brown, K. L.; Hakimi, J. M.; Nuss, D. M.; Montejano, Y. D.; Jacobsen, D. W. *Inorg. Chem.* **1984**, *23*, 1463.
(36) Brown, K. L.; Hakimi, J. M.; Jacobsen, D. W. *J. Am. Chem. Soc.* **1984**, *106*, 7894.
(37) At H = −1, hydrolysis to a mixture of α-ribazole 3′-phosphate and cobinamide phosphate is complete in 42 h.[32]
(38) Allinger, N. L. *J. Am. Chem. Soc.* **1977**, *99*, 8127.
(39) Marques, H. M.; Brown, K. L. *J. Mol. Struct., THEOCHEM* **1995**, *340*, 97.
(40) *HYPERCHEM*, version 4.5; Hypercube Ltd.: 419 Phillip Street, Waterloo, ON, N2L 3X2, Canada.
(41) (a) Bacon, A. D.; Zerner, M. C. *Theor. Chim. Acta* **1979**, *53*, 21. (b) Anderson, W. P.; Edwards, W. D.; Zerner, M. C. *Inorg. Chem.* **1986**, *25*, 2728.
(42) Rossi, M.; Glusker, J. P.; Randaccio, L.; Summers, M. F.; Toscano, P. J.; Marzilli, L. G. *J. Am. Chem. Soc.* **1985**, *107*, 1729.
(43) Kräutler, B.; Konrat, R.; Stupperich, E.; Färber, G.; Gruber K.; Kratky, C. *Inorg. Chem.* **1992**, *33*, 4128.

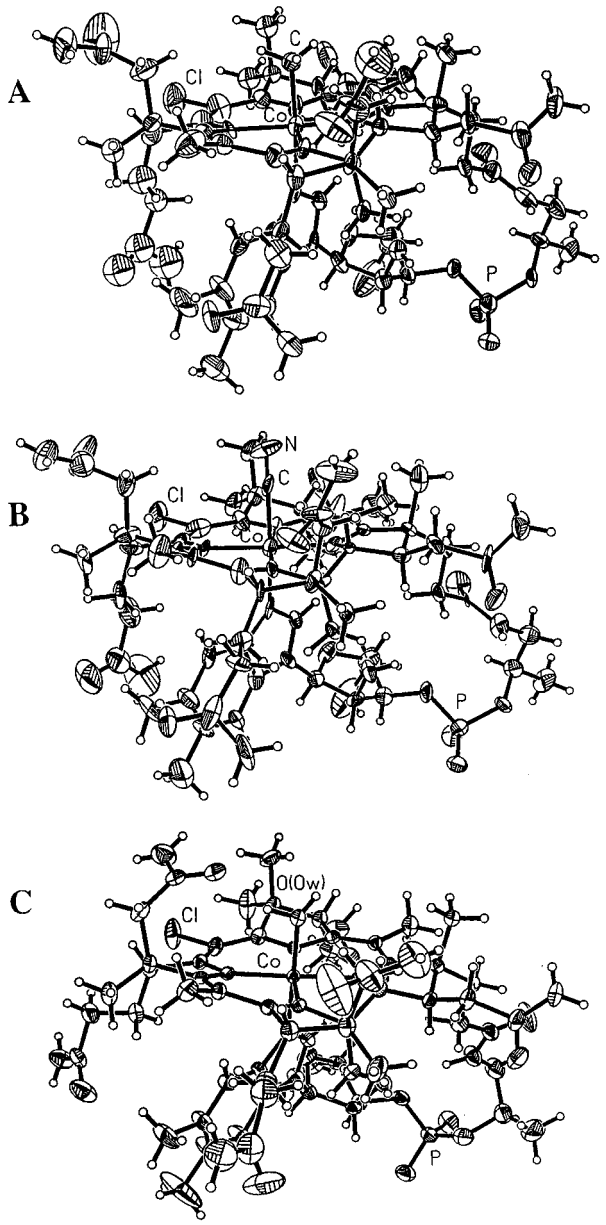

Figure 3. ORTEP diagrams of (A) 10-Cl-MeCbl, (B) 10-Cl-CNCbl, and (C) 10-Cl-H_2OCbl^+. For clarity, only the major conformations are shown.

conversely, the C≡N bond length is shorter (1.09(2) *vs* 1.15(1) Å). As with 10-Cl-MeCbl, the corrin is somewhat less folded and the base is less tilted than in the C10-unsubstituted analog. The disorder in the C ring observed in 10-Cl-MeCbl is also observed in this structure.

Crystal Structure of 10-Cl-$H_2OCbl\cdot ClO_4$. The present structure determination of 10-Cl-$H_2OCbl\cdot ClO_4$ (monoclinic space group $P2_1$, Figure 3C) is among the highest resolution cobalamin structures obtained to date (10 535 independent reflections, $R_1 = 4.3\%$) and is comparable to the structure determination of H_2OCbl^+ itself, performed with a synchrotron radiation source ($R_1 = 5.0\%$).[13] The Co−O bond to coordinated H_2O (1.948(3) Å) is very similar to that found in H_2OCbl^+ (1.952(2)[13] or 1.961(5)[14] Å), but the Co−N3 bond length (1.967(4) Å) is considerably longer (*cf.* 1.925(2)[13] or 1.930(5)[14] Å). The coordinated water molecule is H-bonded to O39 of the *c* side chain amide, and to OP5 of the phosphate of a translational relative; because of the hydrogen bonding, the side chain is oriented over the corrin, rather than in the usual position, pointing outward from the corrin.[44]

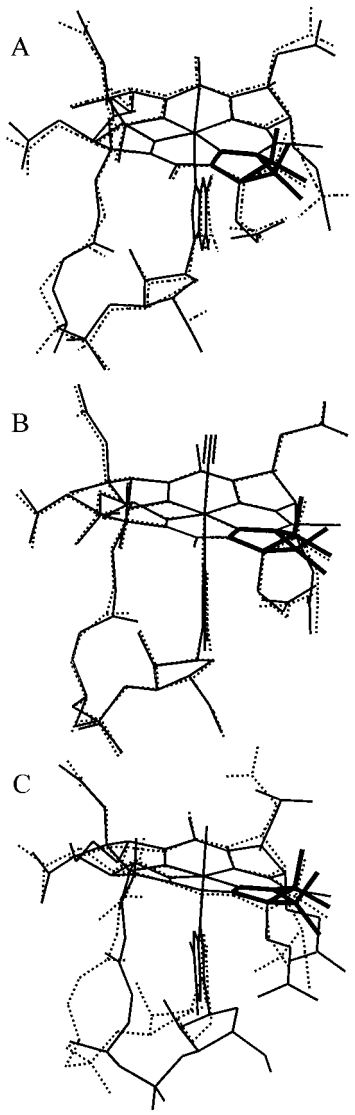

Figure 4. Comparison of the crystal structures of (A) MeCbl (···)[42] and 10-Cl-MeCbl (—), (B) CNCbl (···)[43] and 10-Cl-CNCbl (—), and (C) H_2OCbl^+ (···)[13] and 10-Cl-H_2OCbl^+ (—). The disorder in the C ring of the 10-Cl derivatives is shown with bold lines. The disorder was modeled as the occupation of two conformations of the C ring; in the major conformation, C46 is axial and C47 equatorial, while in the minor conformation, both C46 and C47 are pseudoequatorial and virtually above each other on either side of the mean plane of the C ring.

Because both structures have been determined to high precision, there are many statistically significant bond length and bond angle differences in 10-Cl-H_2OCbl^+ and H_2OCbl^+ (Tables S12 and S13). However, when the comparison is restricted to the same significance level as used in the comparison of MeCbl and 10-Cl-MeCbl (Table S7), there is not a single bond length (and very few bond angles) that is significantly different. The corrin fold angles are also very similar (Table 4). There are, nevertheless, many gross structural differences between the two (Figure 4C). For example, the A ring is a half-chair in both structures but it is somewhat more twisted in 10-Cl-H_2OCbl^+; conversely, the B ring, also a half-chair, is more twisted in H_2OCbl^+ than in 10-Cl-H_2OCbl^+; the C ring is disordered in 10-Cl-H_2OCbl^+ but apparently not in H_2OCbl^+; the D ring is very similarly oriented in both. All of the side chains except for the *a* and *b* side chains have different

(44) Glusker, J. In *B_{12}*; Dolphin, D., Ed.; Wiley: New York, 1982; Vol. 1, p 23.

Table 3. Bond Lengths and Bond Angles of the Coordination Sphere of Co(III) in XCbl and 10-Cl-XCbl (X = Me, CN^- and H_2O)

	MeCbl[a]	10-Cl-MeCbl[b]	CNCbl[c]	10-Cl-CNCbl[b]	H_2OCbl^+ [d]	10-Cl-H_2OCbl^+ [b]
			Bonds/Å			
Co−N21	1.88(2)	1.815(6)	1.875(8)	1.943(13)	1.881(2)	1.886(3)
Co−N22	1.97(2)	1.934(6)	1.908(8)	1.915(11)	1.897(2)	1.912(3)
Co−N23	1.93(2)	1.811(6)	1.917(9)	1.933(12)	1.904(2)	1.929(3)
Co−N24	1.89(2)	1.896(6)	1.875(8)	1.902(12)	1.880(2)	1.892(3)
Co−NB3	2.19(2)	2.200(7)	2.011(10)	2.043(14)	1.925(2)	1.967(4)
Co−C	1.99(2)	1.979(7)	1.858(12)	1.97(2)		
C≡N			1.150(14)	1.10(2)		
Co−O(H_2O)					1.952(2)	1.948(3)
			Angles/deg			
N21−Co−N22	93(2)	89.7(3)	90.4(4)	87.4(5)	90.8(1)	90.3(1)
N24−Co−N23	90(2)	89.4(3)	89.3(4)	88.0(5)	90.9(1)	91.1(1)
N21−Co−N23	172(2)	172.4(3)	172.6(4)	173.6(5)	173.9(1)	174.5(1)
N22−Co−N23	95(2)	97.7(3)	96.8(4)	99.0(6)	95.4(1)	95.2(1)
N22−Co−N24	173(2)	171.6(3)	172.8(4)	171.9(6)	170.9(1)	171.8(2)
N21−Co−N24	81(2)	83.4(3)	83.8(4)	85.7(5)	83.0(1)	83.3(1)
N24−Co−NB3	95(2)	94.3(3)	94.8(4)	94.1(5)	95.3(1)	94.3(1)
N21−Co−NB3	93(2)	92.7(3)	90.7(4)	93.5(5)	91.9(1)	93.1(2)
N22−Co−NB3	89(2)	90.9(3)	89.4(4)	90.6(5)	91.5(1)	91.1(1)
N23−Co−NB3	86(2)	85.3(3)	87.5(4)	86.1(5)	87.8(1)	87.6(2)
N24−Co−C	90(2)	88.8(3)	88.1(4)	88.4(6)		
N21−Co−C	95(2)	93.3(3)	91.7(4)	88.4(7)		
N22−Co−C	86(2)	86.8(3)	87.9(4)	87.1(6)		
N23−Co−C	87(2)	89.1(4)	90.5(4)	92.3(7)		
NB3−Co−C	171(2)	173.6(3)	176.4(4)	176.9(6)		
Co−C−N			179(1)	176(2)		
N24−Co−O					85.5(1)	86.6(1)
N21−Co−O					89.0	87.3(1)
N22−Co−O					87.8(1)	88.0(1)
N23−Co−O					91.4(1)	92.1(1)
NB3−Co−O					178.8(1)	179.1(1)

[a] Reference 42. [b] This work. [c] Reference 43. [d] Reference 13.

Table 4. Corrin Fold Angles and Base Tilt Angles of 10-Cl-MeCbl, 10-Cl-CNCbl, 10-Cl-H_2OCbl^+, and Their C10-H Analogs

complex	corrin fold angle[a]	base tilt angle[b]
10-Cl-MeCbl	14.1	3.7
MeCbl	16.5	4.4
10-Cl-CNCbl	15.1	2.8
CNCbl	18.0	4.9
10-Cl-H_2OCbl^+	18.6	3.1
H_2OCbl^+	18.7	5.5

[a] The dihedral angle angle between the mean plane through N21, C4, C5, C6, N22, C9, and C10 and that through N24, C16, C15, C14, N23, C11, and C10.[44] [b] Half the difference between the two Co−NB3−C angles, *viz.*, $|\theta_{Co-NB3-B9}-\theta_{Co-NB3-B2}|/2$.[43]

orientations, confirming previous observations of the variability of side chain orientations as deduced from an analysis of known crystal structures[44] and from MM studies.[39] We have previously observed, using NOE-restrained MD simulations,[45] that the orientation of the nucleotide loop of the corrins is very variable, and this is observed here. Differences in torsions in the *f* chain, in the aminopropanol group, and around the phosphate have a profound effect on the relative orientations of the ribose and bzm and the corrin ring. The ribose rings have virtually identical orientations in the two complexes, although side chain OR8 is orientated differently. In 10-Cl-H_2OCbl^+ it points downward, away from the rest of the molecule, but it points upward in H_2OCbl^+ and is probably H-bonded to N52 of the *e* side chain amide (OR8···N52 = 2.80 Å).

NMR Observations of XCbl and 10-Cl-X-Cbl (X = Me, CN^-, H_2O). An examination of ^{13}C NMR shifts was undertaken to determine whether the disorder in the C ring in 10-Cl-MeCbl, 10-Cl-CNCbl, and 10-Cl-H_2OCbl^+ persisted in solution. The chemical shifts of C46 and C47 (with C41 as a control), C12 (with C8 as a control), C13 (with C7 as a control), and C48 (with C36 and C37 as controls) in 10-Cl-XCbl and XCbl were compared; the controls are for monitoring the electronic effect of Cl substitution at C10 and are the same number of bonds away from C10, but on the opposite side of the corrin. We also explored the effect of substitution on a number of randomly-selected corrin ring and peripheral carbon atoms and, in addition, surveyed the average chemical shifts for a series of XCbl's (X = AdePr, Ado, CH_3, CN, H_2O, CN-13-*epi*, and CN-8−*epi*) for C46, C47, C12, C13, C48, the control carbon atoms, and randomly selected carbon atoms, to deduce the relative variations of these chemical shifts in the cobalamins. The results are summarized in Table S14 of the Supporting Information.

While the electronic effect of substitution of H by Cl can have a significant effect on the chemical shifts (for example, for C41 $\Delta\delta_1 = \delta_{10-Cl-XCbl}-\delta_{XCbl} = 0.81$, 0.85, and 0.83 ppm for X = Me, CN^-, and H_2O, respectively, while for C7 $\Delta\delta_1 = -0.30$, 0.23, and 0.61 ppm, respectively), the differences between the chemical shifts of C46, C47, C12, and C13 in MeCbl, CNCbl, and H_2OCbl^+ and in XCbl and 10-Cl-XCbl are significantly greater than the electronic effect of substitution (for example, for C12 $\Delta\delta_1 = 2.76$, 2.69, and 2.46 ppm for X = Me, CN^-, and H_2O, respectively). The differences are also significantly larger than differences in the chemical shifts of randomly selected carbon atoms in 10-Cl compounds and a range of cobalamins.

The ^{13}C and ^{15}N shifts in 10-Cl-$^{13}C^{15}N$Cbl are compared with those of free $^{13}C^{15}N^-$ and base-on and base-off $^{13}C^{15}N$Cbl in Table 5. Replacement of H by Cl at C10 causes the ^{13}C resonance of coordinated CN^- to move upfield while the ^{15}N resonance moves downfield.

Molecular Dynamics of 10-Cl-CNCbl. The torsions of the C ring of 10-Cl-CNCbl were monitored during a 100 ps MD

(45) Marques, H. M.; Hicks, R. P.; Brown, K. L. *J. Chem. Soc., Chem. Commun.* **1996**, 1427.

Table 5. ^{13}C and ^{15}N Chemical Shifts in Cyanocobalt Corrins and Free Cyanide Species

compound	cyanide		bzm N atoms, $\delta_{^{15}N}$/ppm[b]	
	$\delta_{^{13}C}$/ppm[a]	$\delta_{^{15}N}$/ppm[b]	B1	B3
CNCbl (base on)[c]	123.6	288.9	163.2	188.3
CNCbl (base off)[c]	114	297.6		
10-Cl-CNCbl	121.8	291.2	164.6	182.3
H_2OCbl^+			166.0	143.6
10-Cl-H_2OCbl^+			169.3	106.9
free CN^-	166.9	272.4		

[a] In DMSO at 27 °C relative to external TSP. [b] Relative to external NH_3(l). [c] Reference 63.

simulation at 300 K to determine whether there was evidence for a ring flip during the simulations. During the simulations the torsions were found to be normally distributed about values very close to those of the major conformation, and there was no evidence of a significant population of the minor conformation.

The pK_as of 10-Cl-MeCbl, 10-Cl-CNCbl, and 10-Cl-H_2OCbl^+. For dissociation of coordinated water in H_2OCbl^+ we found $\Delta H = 36.0 \pm 1.9$ kJ mol^{-1}, $\Delta S = -34 \pm 6$ J K^{-1} mol^{-1}, and pK_a(25 °C) = 8.09 (I = 0.5 M, $NaNO_3$). Differences between the present values and those previously reported[46] ($\Delta H = 28.6 \pm 0.3$ kJ mol^{-1}, $\Delta S = -60 \pm 3$ J K^{-1} mol^{-1}, and pK_a(25 °C) = 8.1, I = 1.0 M, KCl background) may reflect in part the effect of coordination of Cl^- by H_2OCbl^+. For 10-Cl-H_2OCbl^+, $\Delta H = 32.9 \pm 1.5$ kJ mol^{-1}, $\Delta S = -36 \pm 6$ J K^{-1} mol^{-1}, and pK_a(25 °C) = 7.65.

$K_{base-off}$ (eq 3) can be thought of as a combination of the stepwise processes shown as eqs 4 and 5. From the value of $K_{base-off}$ we calculate[47] for 10-Cl-CNCbl $K_{Co} = 4.57 \times 10^3$ ($\Delta G_{Co} = -20.9$ kJ mol^{-1}), compared to 3.35×10^5 ($\Delta G_{Co} = -31.5$ kJ mol^{-1}) for CNCbl itself;[48] and for 10−Cl-MeCbl, $K_{Co} = 181$ ($\Delta G_{Co} = -12.9$ kJ mol^{-1}), compared to 452 ($\Delta G_{Co} = -15.1$ kJ mol^{-1}) for MeCbl itself.[47]

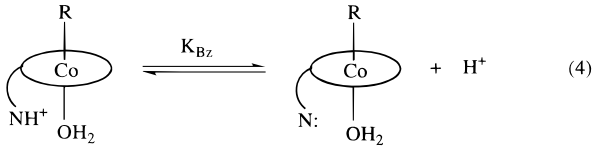

(4)

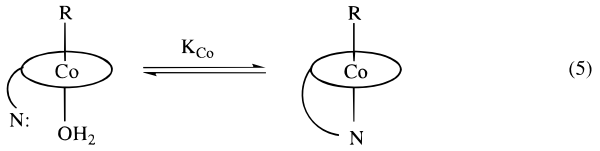

(5)

Discussion

Both 10-Cl-MeCbl and 10-Cl-CNCbl crystallize in the orthorhombic space group $P2_12_12_1$, as found for many cobalt corrins,[44] but the aqua complex crystallizes in the monoclinic space group $P2_1$ instead. This is not without precedent, as both cyanocobalamin-*b*-monocarboxylic acid[49] and cyanoaqua(cobyrinic acid hexaamide)[11] crystallize in this space group. An unusual feature of the structure of all three compounds in the solid state is the disorder in the C pyrrole ring, modeled as a ring flip between a major conformation (C46 axial toward the β face on the corrin as usual, and C47 equatorial) and a minor conformation (C46 and C47 are both pseudoequatorial, respectively above and below the mean plane of the C ring). Although the disorder is apparently not observed in MeCbl,[42] CNCbl,[43] or H_2OCbl^+,[13] the C ring conformation in MeCbl is intermediate between the two conformations observed in 10-Cl-MeCbl (Figure 4C), which suggests that the disorder may have been present in the solid state in MeCbl but was not resolved.

Table 6. Measures of the Donor Power of X in C10-Unsubstituted XCbl's toward Co(III)

axial ligand, X	p$K_{base-off}$	K_{Co}	d_{Co-NB3}/Å
H_2O	−2.13[a]	4.9×10^7	1.925(2)[d]
CN^-	0.11[b]	3.35×10^5	2.011(10)[e]
Me	2.90[c]	4.52×10^2	2.19(2)[f]

[a] Reference 36. [b] Reference 48. [c] Reference 47. [d] Reference 13. [e] Reference 43. [f] Reference 42.

It seems likely that the C ring disorder in the solid state persists in solution as a ring flip, since the differences between the chemical shifts (Table S14) of C46, C47, C12, and C13 in XCbl and in 10-Cl-XCbl are greater than differences in the chemical shifts of randomly selected carbon atoms, and greater also than any electronic effect of substitution of H by Cl (for example, at C41 and C7, although C8 in 10-Cl-H_2OCbl^+ is shifted downfield by 1.83 ppm). In normal XCbl's, the C46 resonance appears near 34 ppm, while the C47 resonance appears near 22 ppm.[27] This has been attributed[27] to steric effects on the the ^{13}C chemical shift[50] since in normal Cbl's the equatorial C47 is crowded by the downwardly pseudoaxial *e* propionamide, while C46 is unencumbered. However, in CN-13-*epi*-Cbl, where C46 is pseudoequatorial and C47 is downwardly pseudoaxial, C46 is crowded by the now upwardly projecting pseudoaxial *e* propionamide and resonates at 22.0 ppm, while C47 is unencumbered and resonates at 32.7 ppm. The observation that in the 10-Cl-XCbl's the ^{13}C chemical shifts of C46 and C47 are considerably closer together ($\Delta\delta \approx 7$ ppm) than in the XCbl's themselves ($\Delta\delta \approx 12$ ppm) suggests that the C ring disorder seen in the solid state persists as a ring flip in solution, with consequent dynamical averaging of the C46 and C47 chemical shifts. Since the line widths of C16, C47, C12, and C13 are very similar to those of other carbon atoms, the flipping motion must be fast on the NMR time scale.[51] As molecular dynamics simulations failed to show any significant population of the minor conformation, this further suggests that an electronic effect from substitution of H by Cl at C10, rather than a steric effect, has decreased the barrier to the ring flip in the C ring.

The ^{15}N and ^1H chemical shifts of the side chain amides of 10-Cl-CNCbl and 10-Cl-H_2OCbl^+ are very similar, with the noteworthy exception of the *c* side chain amide (Table 2), where

(46) Marques, H. M.; Brown, K. L.; Jacobsen, D. W. *J. Biol. Chem.* **1988**, *263*, 12378.
(47) Brown, K. L.; Peck-Siler, S. *Inorg. Chem.* **1988**, *27*, 3548.
(48) Brown, K. L.; Wu, G.-Z. *Inorg. Chem.* **1994**, *33*, 4122.
(49) Edmond, E. D. Ph.D. Thesis, Oxford University, 1970; quoted in ref 45.
(50) (a) Grant, D. M.; Cheney, B. V. *J. Am. Chem. Soc.* **1967**, *89*, 5315. (b) Cheney, B. V.; Grant, D. M. *J. Am. Chem. Soc.* **1967**, *89*, 5319. (c) Schneider, H.-J.; Price, R.; Keller, T. *Angew. Chem., Int. Ed. Engl.* **1971**, *10*, 730. (d) Brietimaier, E.; Voelter, W. *Carbon-13 NMR Spectroscopy;* VCH: Weinheim, Germany, 1989.
(51) If the C ring conformation and C46 and C47 chemical shifts on CN-13-*epi*-Cbl[27] are used as a model for the minor conformation of 10-Cl-CNCbl, those of CNCbl itself are used as a model for the major conformation, and solution populations of the conformers are assumed equal to the site occupancies of 10-Cl-CNCbl in the solid state, then, assuming chemical shift averaging, the calculated chemical shifts for C46 (31.25 ppm) and C47 (24.23 ppm) are remarkably close to those observed for 10-Cl-CNCbl (31.58 and 24.70 ppm, respectively) and the calculated difference in chemical shift between C46 and C47 (7.0 ppm) is essentially the same as the observed difference (6.9 ppm). These simple calculations suggest that CN-13-*epi*-Cbl is indeed a good model for the minor conformation seen in the solid state for the 10-Cl-XCbl's, and that the C ring does undergo a rapid conformational equilibrium in the 10-Cl-XCbl's in solution.

Table 7. Band Positions in the Electronic Spectra of MeCbl, CNCbl, and H_2OCbl^+ and Their 10-Cl Analogs and Partial Charges from a MPA on Chlorine and Cobalt

compound	band position/nm				partial charge/e	
					on chlorine[a]	on cobalt[a]
MeCbl	266, 280, 290	316, 342, 357, 375 (sh)	484 (sh)	518		−0.158
10-Cl-MeCbl	285, 291	367, 374	500 (sh)	543	−0.328	−0.148
CNCbl	304, 322	360.5	517	551		−0.109
10-Cl-CNCbl	282, 289	364	546	576	−0.282	−0.148
H_2OCbl^+	275	351	495	524		0.006
10-Cl-H_2OCbl^+	280	357	527	554	−0.266	−0.008

[a] From a semiempirical MO calculation at the solid state geometry using the ZINDO/1[41] model.

both ^{15}N and ^{1}H resonances are shifted downfield in 10-Cl-H_2-$OCbl^+$ relative to 10-Cl-CNCbl. This is diagnostic of an H bond from a donor (in this case, the coordinated H_2O) to the amide carbonyl oxygen.[52] The hydrogen bond between coordinated H_2O and the amide carbonyl oxygen of the *c* side chain amide, which appears to persist in solution, has been previously observed in the crystal structures of H_2OCbl^+ [13,14] and in aquacyanocobyric acid;[11] it may prove to be a general feature of all corrins with water coordinated in the β coordination site of Co(III).

The number of significant differences in bond lengths and bond angles between 10-Cl-XCbl and XCbl depends on X (Table S7). If the comparisons are confined to bonds and angles within the corrin ring (since groups on the periphery are involved in different patterns of hydrogen bonding and are likely to be subjected to different packing forces in the solid state), there are 18 bond lengths and 25 bond angles that are significantly different between MeCbl and 10-Cl-MeCbl; 5 and 11, respectively, between CNCbl and 10-Cl-CNCbl; and 0 and 2, respectively, between H_2OCbl^+ and 10-Cl-H_2OCbl^+. As X is changed from H_2O, to CN^-, to Me, the corrin ring becomes more flexible to deformation. This is clearly an electronic effect as all three ligands are very small and are unlikely to have a significant steric influence on the corrin structure. The electronic influence of the ligand X may be assessed from the values of K_{Co} (or $pK_{base-off}$, Table 6) in C10-unsubstituted XCbl's. K_{Co} decreases and d_{Co-NB3} increases (XCbl becomes more "base-off") as the donor power of X increases in the series H_2O < CN^- < Me. These effects are in agreement with the relative positions of these ligands in the *trans* influence order of ligands in the cobalt corrins.[53,54] We conclude that the flexibility of the corrin ring increases with the donor power of the axial ligand.

The substitution of H by Cl at C10 causes $pK_{base-off}$ to increase, but the absence of a value for 10-Cl-H_2OCbl^+ makes it impossible to draw firm conclusions concerning the trends. The effect is more marked for 10-Cl-CNCbl than for 10-Cl-MeCbl ($\Delta pK_{base-off}$ = 1.86 and 0.40, respectively), consistent with a significant change in d_{Co-NB3} for the former, but not the latter, on C10 substitution.

The UV−visible spectra of the cobalt corrins are dominated by $\pi-\pi^*$ transitions of the 14-electron π system.[55] The band positions are sensitive to the axial ligands and substituents on the periphery of the corrin ring.[56] It is known that strong donor ligands cause the electronic transitions to shift to lower energy as the charge density on the metal ion and hence, presumably, in the π system increases,[56,57] and the band positions correlate with the ligand position in the nephelauxetic series.[57] Substituents on the corrin can cause a direct perturbation of the charge density in the π system. The bands of CN_2Cbl^- (367, 540, 580 nm) shift to 369, 561, and 602 nm and to 370, 561, and 602 nm on chlorination[58] and bromination,[59] respectively, at C10 but to 354, 415, and 530 nm on nitrosation, while the 10-amino derivative is reported to have a deep blue color.[59] This is consistent with Cl, Br, and NH_2 acting as electron donors toward the corrin, and NO as an electron acceptor. We find that chlorination at C10 in MeCbl, CNCbl, and H_2OCbl^+ causes a shift in the band positions to longer wavelength (Table 7). Thus although chlorine is an inductively electron withdrawing substituent,[60] its resonance electron donation is the more important effect on electron distribution in the corrin ring.

The axial ligand, X, and chlorine at C10 are competitive electron donors toward the delocalized π electron system of the corrin ring. As the donor ability of X increases (H_2O < CN^- < Me), the ability of Cl to act as a resonance donor decreases, as seen by the response of the C10−Cl bond length to the identity of X. The average C(sp^2)−Cl and C(aromatic)−Cl bond lengths observed crystallographically are 1.734(19) and 1.739(0.010) Å, respectively.[61] In 10-Cl-XCbl, d_{C10-Cl} is 1.745-(4) Å (X = H_2O), 1.77(2) Å (X = CN^-), and 1.816(10) (X = Me), *i.e.*, d_{C10-Cl} increases from a "normal" value as the donor power of X increases. There are very good correlations (not shown) between $pK_{base-off}$ of XCbl and d_{C10-Cl} in 10-Cl-XCbl (R^2 = 0.994), and between d_{Co-NB3} in XCbl and d_{C10-Cl} in 10-Cl-XCbl (R^2 = 0.999).

It is generally accepted that the arbitrary procedures used for assigning partial charges to atoms from a Mulliken population analysis (MPA) compromise their reliability, not least because of the basis set dependence of the values.[62] Nevertheless, the procedure may provide useful information if used in a consistent manner, for example, when comparing similar structures under the same conditions. We thus find that the partial charges obtained from applying the ZINDO/1 model[41] to MeCbl, CNCbl, H_2OCbl^+, and their 10-Cl analogs correlate reasonably well with

(52) (a) Krauss, E. M.; Chan, S. I. *J. Am. Chem. Soc.* **1982**, *104*, 6953. (b) Shafer, R. H.; Formica, J. V.; Delfini, C.; Brown, S. C.; Mirau, P. A. *Biochemistry* **1982**, *21*, 6496. (c) Llinas, M.; Horsley, W. J.; Klein, M. P. *J. Am. Chem. Soc.* **1976**, *98*, 7554. (d) Williamson, K. L.; Pease, L. G.; Roberts, J. D. *J. Am. Chem. Soc.* **1979**, *101*, 714.
(53) Pratt, J. M. *The Inorganic Chemistry of Vitamin B_{12}*; Academic Press: London, 1972.
(54) Firth, R. A.; Hill, H. A. O.; Pratt, J. M.; Thorp, R. G.; Williams, R. J. P. *J. Chem. Soc. A* **1968**, 2428.
(55) (a) Day, P. *Coord. Chem. Rev.* **1967**, *2*, 109. (b) Offenhartz, P. O.; Offenhartz, B. H.; Fung, M. M. *J. Am. Chem. Soc.* **1970**, *92*, 2966. (c) Veillard, A; Pullman, B. *J. Theor. Biol.* **1965**, *8*, 307. (d) Schrauzer, G. N; Lee, L. P.; Sibert, J. W. *J. Am. Chem. Soc.* **1970**, *92*, 2997. (e) Salem, L.; Eisenstein, O.; Anh, N. T.; Burgi, H. B.; Devaquet, A.; Segal, G.; Veillard, A. *Nouv. J. Chim.* **1977**, *1*, 335.
(56) Giannotti, C. In *B_{12}*; Dolphin, D., Ed.; Wiley: New York, 1982; Vol. 1, p 393.
(57) Schrauzer, G. N. *Naturwissenschaften* **1969**, *53*, 459.
(58) Wagner, F; Bernhauer, K. *Ann. N.Y. Acad. Sci.* **1964**, *112*, 580.
(59) Wagner, F. *Proc. R. Soc. London, Ser. A* **1965**, *A288*, 344.
(60) Ehrenson, S.; Brownlee, R. T. C.; Taft, R. W. *Prog. Phys. Org. Chem.* **1973**, *10*, 1.
(61) Allen, F. H.; Kennard, O.; Watson, D. G.; Brammer, L.; Orpen, A. G.; Taylor, R. *J. Chem. Soc., Perkin Trans. 2* **1987**, S1.
(62) Bachrach, S. M. In *Reviews in Computational Chemistry*; Lipkowski, K. B., Boyd, D. B., Eds.; VCH Publishers: New York, 1994; Vol. 5, p 171.

^{13}C NMR chemical shifts (Figure S1 of the Supporting Information), indicating that nuclear shielding increases with an increase in charge density.

Substitution of H by Cl at C10 causes an increase in charge density at Co when X = H_2O and CN^-, but a decrease when X = Me (Table 7); conversely, the partial charge on chlorine increases as the donor power of X increases. The coordination sphere of the metal responds and d_{Co-NB3} increases when X = H_2O and CN^-, but remains unchanged when X = Me. There is virtually no change in the average partial charge on the four equatorial N donor atoms of the corrin when X = H_2O (−0.177 in H_2OCbl^+, −0.174 in 10-Cl-H_2OCbl^+) or X = CN^- (−0.175 in CNCbl, −0.179 in 10-Cl-CNCbl), and the Co−N equatorial bond lengths change very little (an average lengthening by 0.01 Å from H_2OCbl^+ to 10-Cl-H_2OCbl^+; and a lengthening by 0.03 Å from CNCbl to 10-Cl-CNCbl), but decrease by an average of 0.05 Å from MeCbl to 10-Cl-MeCbl as the average partial charge on the equatorial N donor atoms decreases from −0.187 to −0.165.

The pK_a for coordinated water is lower in 10-Cl-H_2OCbl^+ than in H_2OCbl^+ (7.65 compared to 8.08). There is no change in d_{Co-O}, however, possibly because of the anchoring of the axial ligand by hydrogen bonding to the *c* amide side chain. The decrease in pK_a is consistent with a lower charge density on oxygen in the hydroxo complexes of 10-Cl-HOCbl (−0.456) compared to that in HOCbl (−0.503) as revealed by a MPA on the two complexes using the ZINDO/1 model.

A consequence of the increased Co−C bond length in 10-Cl-CNCbl is a concomitant decrease in the C−N bond length of coordinated cyanide and is explained if metal−cyanide dπ−pπ bonding is important in cyanocobalamins, as in eq 6. Poorer

$$Co-C\equiv N \leftrightarrow Co^+=C=N^- \qquad (6)$$

dπ−pπ bonding would cause the Co−C bond length to increase and, consequently, the C−N bond length to decrease. The importance of dπ−pπ bonding in cobalt corrins and cobaloximes has previously been demonstrated.[63,64] The chemical shifts (Table 5) of 10-Cl-$^{13}C^{15}N$Cbl are in accord with the structural changes. Apparently due to dπ−pπ back-bonding, the ^{13}C and ^{15}N chemical shifts of the cyanide ion have been shown to move in opposite directions when cyanide is coordinated to cobalt in corrins, and when the *trans* ligand is altered in cyanocobalt corrins.[63] Here we find that chlorination of CNCbl at C10 also causes the cyanide ^{13}C resonance to shift upfield and the ^{15}N resonance to shift downfield. Hence, their chemical shifts are consistent with a weaker axial Co−N_{B3} bond in 10-Cl-CNCbl than in CNCbl itself.

The ground state structural effects observed in 10-Cl-XCbl's are in consonance with the kinetic effects previously referred to (Table 1). A picture is beginning to emerge of the *cis* electronic effects in the cobalt corrins from substitution in the axial coordination site and on the corrin ring. We are exploring these effects further and will report on our results elsewhere.

Conclusions

Substitution of H by Cl at C10 has a number of structural, thermodynamic, and electronic consequences:

(a) There is disorder in the C ring which was resolved by a two-site occupancy model; in the major conformation C46 occupies its usual axial position and C47 is equatorial, and in the minor conformation both C46 and C47 are in pseudoequatorial positions. NMR observations suggest that the disorder may persist in solution as a ring flip. Since molecular dynamics simulations fail to reveal any significant population of the minor conformation, the origin of the disorder is likely to be an electronic effect from substitution at C10.

(b) The bonds to the equatorial N donors, C−N_{eq}, are significantly shorter in 10-Cl-MeCbl than in MeCbl; in 10-Cl-CNCbl the Co-C bond is longer and the C−N bond of coordinated CN^- is shorter than in CNCbl; and in 10-Cl-H_2-$OCbl^+$ the Co−NB3 bond is longer than in H_2OCbl^+.

(c) As the donor power of X increases (H_2O < CN^- < Me), the number of bond lengths and angles that differ significantly between 10-Cl-XCbl and XCbl increases, and the C10−Cl bond length increases as well.

(d) K_{Co}, the equilibrium constant for coordination of bzm to Co(III), is smaller in 10-Cl-XCbl than in XCbl (X = Me, CN^-); K_{Co} could not be determined for 10-Cl-H_2OCbl^+ because of competing phosphodiester hydrolysis.

(e) There is an increase in electron density in the π conjugated system causing the bands in the electronic spectrum to move to lower energy.

(f) Semiempirical MO calculations using the ZINDO/1 model show an increase in charge density on Co for X = H_2O and CN^- while the charge density on the equatorial N donors remains virtually unchanged, but they show a decrease when X = Me while the charge density on N(eq) increases. The perturbation in charge distribution is consistent with the observed changes in the axial and equatorial bond lengths to the metal ion.

(g) The charge density on Cl increases as the donor power of X increases.

These observations are all consistent with competitive electron donation onto the corrin macrocycle by the axial donor X, and the corrin substituent, Cl, for which resonance electron donation is a more important effect than inductive electron withdrawal.

Acknowledgment. This work was supported by the donors of the Petroleum Research Fund, administered by the American Chemical Society (Grant 28506-AC3) (K.L.B.), and the Foundation for Research Development, Pretoria, and the University of the Witwatersrand through the Centre for Molecular Design (H.M.M.).

Supporting Information Available: Tentative ^{13}C NMR assignments for 10-Cl-MeCbl, 10-Cl-CNCbl-*c*-lactone, 10-Cl-CNCbl-*c*-COO^- and 10-Cl-H_2OCbl^+ and complete ^{13}C NMR assignments for 10-Cl-CNCbl, amide ^1H and ^{15}N chemical shifts for 10-Cl-CNCbl-*c*-COO^- and 10-Cl-CNCbl, correlation table for the NMR connectivities of 10-Cl-CNCbl observed by COSY, HOHAHA, ROESY, and HMBC spectroscopies, ^{13}C and ^1H NMR assignments for 10-Cl-CNCbl, correlations between atomic partial charges from a MPA analysis on CNCbl and 10-Cl-CNCbl, crystal and structural refinement data for 10-Cl-MeCbl, 10-Cl-CNCbl and 10-Cl-$H_2OCbl\cdot ClO_4$, significant differences in bond lengths and bond angles between XCbl and 10-Cl-XCbl (X = Me, CN^-, H_2O) arranged in order of decreasing absolute magnitude, comparison of bond lengths and bond angles in MeCbl and 10-Cl-MeCbl, in CNCbl and 10-Cl-CNCbl, and in H_2OCbl^+ and 10-Cl-H_2OCbl^+, ^{13}C NMR chemical shift comparison of 10-Cl-XCbl to XCbl and to average chemical shifts (X = Me, CN^-, H_2O), tables of atomic coordinates, anisotropic temperature factors, bond angles, and bond distances, calculated hydrogen atom coordinates, and intermolecular contacts for the crystal structure of 10-Cl-MeCbl, 10-Cl-CNCbl, and 10-Cl-$H_2OCbl\cdot ClO_4$, and ORTEP diagrams showing the disorder in the C ring in 10-Cl-XCbl (X = Me, CN^-, H_2O) (128 pages). Ordering information is given on any current masthead page.

(63) Brown, K. L.; Gupta B. D. *Inorg. Chem.* **1990**, *29*, 3854.
(64) Brown, K. L.; Satyanarayana, S. *Inorg. Chem.* **1992**, *31*, 1366.

IC9615077